

A LOW ENERGY VAN DE GRAEFF ACCELERATOR FOR THE STUDY OF SEMICONDUCTOR DETECTOR SURFACES AND OF THE STOPPING POWER OF BIOLOGICAL MATERIALS

A.K.M.M. Haque, Ph.D., F.Inst.P.,
Department of Physics
University of Petroleum & Minerals
Dhahran, Saudi Arabia

SUMMARY

A proton beam stable at energies upto 400 KeV has been obtained by attenuation due to back-scattering from a gold layer on a Be substrate and by collimation. The beam has been used to measure the window thicknesses of silicon surface barrier detectors and the stopping power of tissue - equivalent materials. The window thickness measurements are part of an investigation of dead layer characteristics; in addition, this is an important correction to energy loss measurements for the stopping power work. Silicon detectors are fabricated as part of a study of the effect of surface treatments on detector characteristics. Three different processes of oxidation are being employed on Si surface after polishing and etching. The stopping power work is part of a study of the effect of phase of tissue-equivalent materials with regard to the dosimetry of fast neutrons.

INTRODUCTION

Particle accelerators are being increasingly used in fields other than nuclear physics - biology and medicine being no exception. The work described in this paper follows from our interest in the stopping power for alpha particles since middle sixties¹ for the dosimetry of the daughter products of radon. There has been greater urgency for further studies because of the acceleration of Nuclear Power Programme, for example, Radiation Protection Programme of E.E.C.² The other fields which are equally important concern the applications of the stopping power results for the dosimetry of fast neutrons for protection and therapy^{3,4}. In our scheme of work, the study of the semiconductor detectors and of the stopping power of tissue-equivalent materials have proceeded side by side. This is due to the fact that we have felt that accurate knowledge of the properties of the semiconductor detectors used for the stopping power work is important; indeed, in order to be able to characterise a detector adequately other properties of importance are energy resolution, ruggedisation, leakage current etc.

PROTON BEAM FROM THE VAN DE GRAEFF ACCELERATOR

The beam transport arrangements have been described earlier⁵. The accelerator provides stable beams in the range 2-20 μ A, but to obtain satisfactory performance of the surface barrier detector spectroscopy system, the beam intensity has been attenuated by a factor of 10^{10} by employing Rutherford scattering at 90° and collimation. The Rutherford scattering takes place from a 20 nm thick evaporated gold film on a beryllium substrate. A magnet deflects the proton beam into one of two beam lines, containing targets for performing (p, γ) resonance experiments for energy calibration; the second line contains the arrangement for detector and stopping power studies.

STUDY OF THE SEMICONDUCTOR DETECTOR SURFACES WITH PROTON BEAMS

Silicon semiconductor detectors are widely used for the detection of charged particles, which enter the detector via a gold electrode, a silicon dioxide layer and a variable dead layer, where the charge collection is inhibited. The major limitation in using these detectors with low energy and highly ionising particles is the energy lost in the above layers taken together i.e. the window. This complicates the energy response of the detector, making it non-linear with pulse-height and also increasing the energy spread of the pulses due to straggling etc. in the window.

The window thickness may be divided into two distinct regions; a fixed part, the gold and silicon dioxide layers and the variable dead layer, often found dependent on detector bias and silicon resistivity. The structure of the window of the semiconductor detector is intimately related to the surface conditions, giving rise to a wide variety of dead layer phenomena. The effect of the surface treatment on the window has not yet been fully investigated and the nature of the dead layer can only be defined by understanding the charge collection process inside the detector. This requires the construction of a range of detectors employing various surface treatments and the investigation of their properties. The performance of both resolution and window thickness with bias voltage and temperature must be measured in addition to their diode characteristics. In the present study the gold and silicon dioxide layer thickness are found during the evaporation process and by ellipsometry, respectively. The total thickness measured with proton beams is then related to theoretically available window models.

The window of the detector is the section traversed by protons in which they lose energy that does not contribute to the pulse height. What is measured experimentally, is the pulse height defect, the difference between the measured pulse height and predicted pulse height if the particle gave up all its energy in creating e-h pairs.

Previous window thickness studies⁶ used the difference in pulse heights obtained from 80 KeV protons and 80 KeV γ -rays to determine the energy lost in the window. The present technique compared the pulse heights due to protons incident at 45° and perpendicularly as follows: Fig.1. A particle of energy E_0 , incident normally ($\theta = 0^\circ$) to the detector surface loses an energy ΔE_0 ; $\Delta E_0 = (dE/dX) X_w$, where X_w is the thickness of the window. The energy lost for an angle of incidence θ is $\Delta E_\theta = E_0/\cos \theta$. The difference between the measured pulse heights is $\Delta E_0 \{ (1/\cos \theta) - 1 \}$

The window thickness of various detectors have been measured by this method using protons (as well as α -particles from an Am-241 source); the fixed part of the window, the gold and silicon dioxide layers have been determined during gold evaporation and by ellipsometry respectively.

The pulse height spectra have been fitted with a gaussian plus exponential function⁷ (Fig.2) in order to extract objective values for the peak shift and $fwhm$. These measurements confirm the existence of a dead layer which is both bias and temperature dependent. The surface conditions of these detectors have been changed during the manufacture by employing different processing techniques. These surface conditions are characterised by high frequency C-V curves from which the barrier height has been determined. Processing differs at the oxidation stage; one set is prepared by exposing the silicon slices to oxygen gas bubbled through distilled water for two weeks and the other set by immersing them in 1% potassium dichromate solution at 70°C for 30 minutes. The resulting surface conditions are characterised by a plot of C^{-2} vs V which gives an intercept of $(V_{do} - \frac{kt}{e})$ on negative V -axis (Fig.3), where V_{do} is the diffusion potential and kt is 0.025 eV. These intercepts have a value approximately 0.45 V for the slices treated with wet oxygen and 2-4 V for those dichromated. The measured dead layer thicknesses have been compared with the theoretical predictions due to models of Caywood et al⁸, Siffert et al⁹, and Hansen¹⁰.

The principle of trapping and recombination was used by Caywood et al as the basis for their model of window thickness. They assumed carrier diffusion effects to be the over-riding factor in determining the window thickness. Electronics which diffuse against the drift field will be lost and not contribute to pulse height. The distance over which the diffusion effects dominate is the distance in which the potential changes by kT/e .

Siffert et al considered the possibility that the rectifying junction is created by a diffusion of oxygen ions into the bulk semiconductor, where they act as acceptors. Undepleted acceptors are considered to act as traps or recombination centres causing complete loss of charge in the p-type layer. Analysis of the space charge conditions gives the thickness of the window.

The success of the oxygen diffusion model certainly indicates that the window thickness is strongly tied to the thickness of the p-type layer at the surface. Also, the shape of the barrier will be similar in the case of an inversion layer to that obtained in the diffused oxygen model. However, in the inversion layer, the dominant charge loss mechanism is regarded to be recombination in the dense electron-hole plasma created along the track of the particle. This situation was considered by Hansen. The inversion layer at the surface constrains the carriers to move in a deep potential well, thus giving rise to a reduction in mobility due to diffuse scattering at the surface. Thus the charge carriers diffuse away much less rapidly in this region, giving rise to a bottle-shaped charge distribution (Fig.4). Calculations of surface mobility and p-layer thickness show favourable agreement with window thickness measurements (Fig.5). Despite excellent agreement, other mechanisms of trapping and recombination at the surface cannot be ignored. Also, a comprehensive model of the window must consider the charge collection process as a function of depth within the barrier.

The study of the stopping power of tissue-equivalent materials for protons and alpha particles is important firstly to provide accurate values and secondly to investigate the phase effect for the dosimetry of neutrons in connection with therapy and radiation protection. We have been interested in the stopping power of alpha particles since middle sixties in connection with the dosimetry of radon daughter products, but this has been further strengthened because of renewed interest in the subject due to Nuclear Power Programme.

Polymer films are often used as tissue-equivalent media; in our programme of work we have chosen polyethylene, polypropylene and polystyrene for the stopping power and associated measurements with protons and this paper presents some results on polyethylene films. The second stage of the study consists of similar measurements with the gaseous phase viz., ethylene, propylene and acetylene, for which experimental arrangement is nearly ready. These films are prepared by us in preference to commercial ones, whose uniformity of thickness is not acceptable. The films are fabricated by slowly withdrawing optically flat glass plates, aluminised for VAMFO examination, from molten solutions. A dust-free enclosure is essential and part-drying of the films is carried out in a temperature-controlled environment. The thickness and uniformity of the films are checked by VAMFO (Variable Angle Monochromatic Fringe Observation) technique before transfer to metallic segments for mounting on the target holder; the thickness of the mounted film is again measured with a Michelson Interferometer.

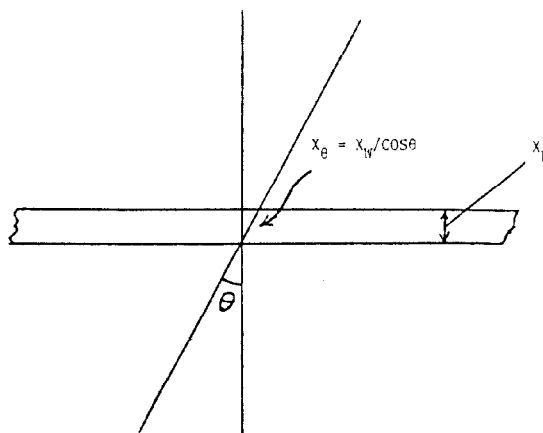
The stopping power of the films has been measured by examining the proton beam before and after its passage through these. The film samples are mounted on a target holder, which can be rotated from outside, containing seven films and one blank. The proton spectrum has been fitted with a computer programme (Fig.2). From the measured values of $-dE/dx$ for polyethylene, the average value of the stopping cross-section for a CH_2 group (for energy loss less than 20%) is $14.4 \times 10^{-15} \text{ eV} \cdot \text{cm}^2$, which is in agreement with Sautter and Zimmermann¹¹.

The straggling of energy loss of heavy charged particles is another important phenomenon which needs careful investigation from dosimetric considerations. Various theories have been put forward which are partially successful and that only in cases of low energy losses. Bohr¹² originally gave the variance as $\Omega^2 = 4\pi Z_1^2 Z_2 e^4 Nt$, which has been modified by Lindhard and Scharff¹³ to take into account energy losses of low and medium energy particles. Bonderup and Hvælpund¹⁴ and Chu¹⁵ have refined Lindhard and Scharff's model. More recently, Soefield et al¹⁶ claimed excellent agreement of the straggling of alpha particles in aluminium with Bethe-Livingston Theory. Besenbacher et al¹⁷ have discussed energy straggling for protons and alpha particles with special emphasis on correlation effects resulting from the bunching of electrons in atoms and molecules. Agreement of measured values with the theory is claimed to be good in gases, results being obscure in solids. These authors have considered energy losses which are 10% or less of the initial energy. Our interest necessarily includes higher energy losses. The only satisfactory theory for high energy losses is at present due to Tschalar¹⁸, with which our results show reasonable agreement.

REFERENCES

1. Haque, A.K.M.M., Proc. Conf. Computational Physics, 33.1 - 33.10, Culham, UKAEA, 1969.
2. Commission of the European Communities, Radiation Protection Programme (1980-1984), Brussels, 1979.
3. International Commission on Radiation Units and Measurements, ICRU Report 27, 1978.
4. Holt, P.D. (Ed.), Biomedical Subcommittee, U.K. Nuclear Data Committee, Physics Med. Biol., 24, 1-17, 1979.
5. Haque, A.K.M.M., Hasko, D.G., Nikjoo, H., Mohammadi, A., Proc. Int. Conf. Low Energy Ion Beams, University of Bath, Institute of Physics, 48-53, 1980.
6. Forcinal, G., Siffert, P. and Coche, A., IEEE Trans. Nucl. Sc., NS-15, No.1, 475-80, 1968; No.3, 275-80, 1968.
7. Baba, H., Nucl. Instrum. Meth., 148, 173-8, 1978.
8. Caywood, J.A., Mead, C.A. and Mayer, J.W. Nucl. Instrum. Meth., 79, 329-32, 1970.
9. Siffert, P., Forcinal, G. and Coche, A. IEEE Trans. Nucl. Sc., NS-14, No.1, 532-6, 1967.
10. Hansen, N.J., Nucl. Instrum. Meth., 96, 373-81, 1971.
11. Sautter, C.A., and Zimmerman, E.J., Phys. Rev., 140, A490-8, 1965.
12. Bohr, N., K. Danske Vidensk. Selsk., Mat.-Fyz, Meddr, 18, 1-144, 1948.
13. Lindhard, J. and Scharff, M., K. Danske Vidensk. Selsk., Mat.-Fys. Meddr., 27, 1-31, 1953.
14. Bonderup, E. and Hvelplund, P., Phys. Rev., A4, 562-9, 1971.
15. Chu, W.K., Phys. Rev., 13A, 2057-60, 1976.
16. Sofield, C.J. Cowern, N.E.B., Freeman, J.M. and Parthasaradhi, K., Phys. Rev., 15A, 2221-6, 1977.
17. Besenbacher, F., Andersen, J.U., and Bonderup, E., Nucl. Instrum., Meth., 168, 1-15, 1980.
18. Tschalar, C., Nucl. Instrum. Meth., 61, 141-8, 1968.

CHARGED PARTICLES



$$\Delta E_{\theta} = X_{\theta} \frac{dE}{dX} = \frac{\Delta E_0}{\cos \theta}$$

FIG. 1 ENERGY LOSS IN THE WINDOW

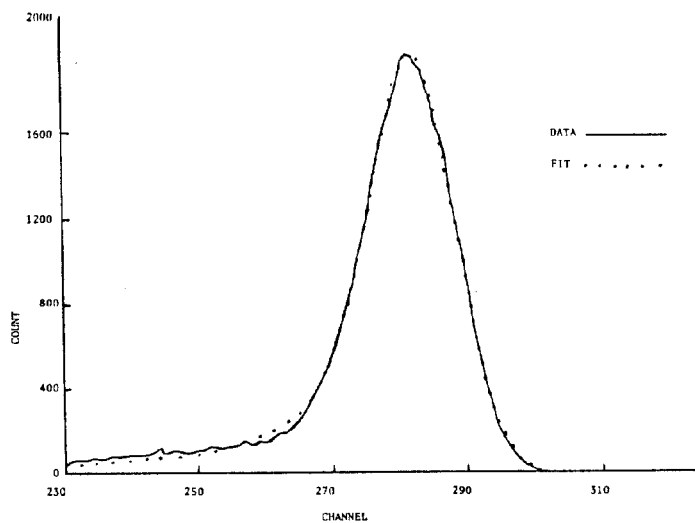


FIG. 2 PROTON SPECTRA; 1.1 MICRON FILM

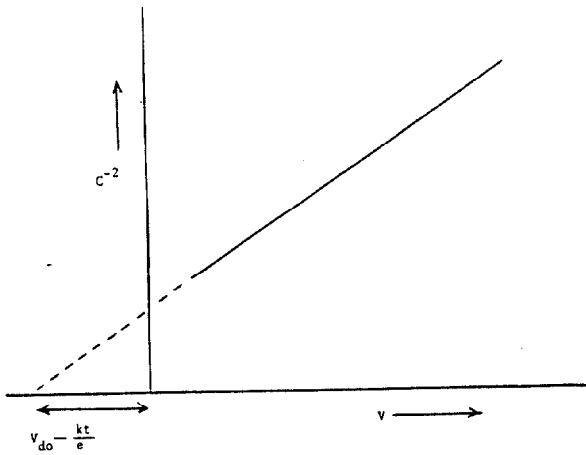


FIG. 3 C^{-2} VS. V PLOT

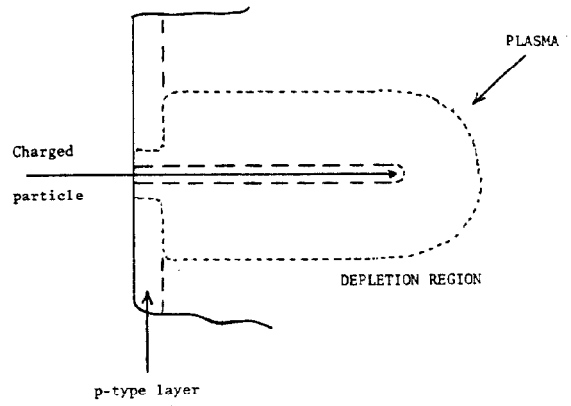


FIG. 4 BOTTLE SHAPED CHARGE DISTRIBUTION

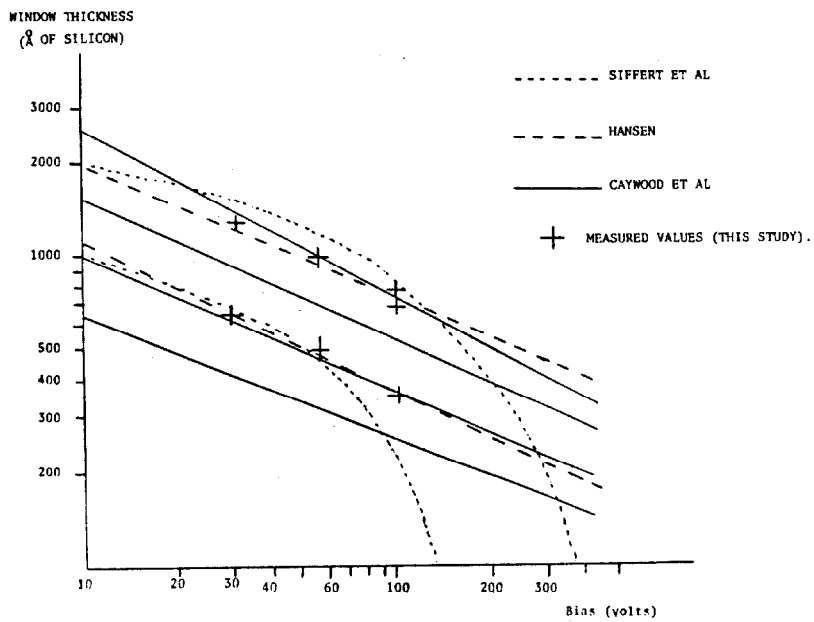


FIG. 5 WINDOW THICKNESS MODEL PREDICTIONS